Applicability of the Langmuir Equation of State for Asphaltene Adsorption at the Oil–Water Interface: Coal-Derived, Petroleum, and Synthetic Asphaltenes

8 AUTHORS, INCLUDING:

Jayant Rane
City College of New York
7 PUBLICATIONS **127** CITATIONS

SEE PROFILE

Vincent Pauchard
SINTEF
18 PUBLICATIONS **228** CITATIONS

SEE PROFILE

Oliver C Mullins
Schlumberger Limited
245 PUBLICATIONS **5,971** CITATIONS

SEE PROFILE

Andrew E Pomerantz
Schlumberger Limited
81 PUBLICATIONS **1,283** CITATIONS

SEE PROFILE

Applicability of the Langmuir Equation of State for Asphaltene Adsorption at the Oil–Water Interface: Coal-Derived, Petroleum, and Synthetic Asphaltenes

Jayant P. Rane,[†,‡,⊥] Sharli Zarkar,[†,‡,⊥] Vincent Pauchard,[‖,⊥,†,‡,#] Oliver C. Mullins,[§] Dane Christie,[‡] A. Ballard Andrews,[§] Andrew E. Pomerantz,[§] and Sanjoy Banerjee*[,†,‡,‖]

[†]Energy Institute and [‡]Department of Chemical Engineering, City College of New York, New York, New York 10031, United States
[§]Schlumberger-Doll Research, Cambridge, Massachusetts 02139, United States
[‖]Flow Technology Group, Department of Process Technology, SINTEF Materials and Chemistry, Trondheim, Norway
[⊥]FACE, the Multiphase Flow Assurance Innovation Center, Norway

Ⓢ Supporting Information

ABSTRACT: In recent studies of asphaltenes from the Norwegian continental shelf at water–oil interfaces, adsorption from largely aliphatic oils appeared to be governed at early times by molecular diffusion and at later times by molecular random sequential adsorption. In addition, the interfacial tension of asphaltenes at the oil–water interface was a a unique function of interfacial coverage, and no apparent rearrangement of asphaltenes at the interface was observed within an experimental time frame of up to 12 h. Confirmation of this result was obtained by showing that high frequency elasticity is a unique function of asphaltene interfacial tension. Both interfacial tension versus coverage and elasticity versus interfacial tension data have been successfully captured by the Langmuir Equation of State (EoS), which also allows estimates of the sizes of the asphaltene polyaromatic cores to be made. The value obtained in experiments with asphaltenes from a Norwegian crude oil is 0.32 nm²/molecule, which corresponds to an average size of ~6.2 ring polyaromatic core resting flat on the oil–water interface, which is supported by estimates made by other means. In the current study, we provide further investigation of these findings. UG8 asphaltenes, which have been well-studied previously, show interfacial behavior similar to the asphaltenes from the Norwegian oil. Experiments with coal-derived asphaltenes, which are known to have smaller cores, and model asphaltenes, with a larger cores, both confirm the applicability of the Langmuir EoS to fit the interfacial tension data and enable estimates of the polyaromatic core sizes from tensiometric measurements.

1. INTRODUCTION

Emulsion stability is a key issue in oil production processes. Indigenous components of crude oils such as resins,[12] waxes, and inorganic particles[3−5] stabilize emulsions and hinder separation of the oil from produced water. Asphaltenes, a class of alkylated polyaromatic hydrocarbons that naturally occur in crude oil, are a major emulsion stabilizer.[6−9] Recent tensiometric experiments have shed light on the behavior of asphaltenes at the oil–water interface.[10−14] Using the pendant droplet experiments and using them to emulate a Langmuir trough, surface tension of asphaltene laden interfaces has been shown to scale with surface coverage independent of aging time, oil viscosity, and asphaltene concentration, both below and above the critical nano-aggregation concentration (CNAC).[10,11] The fact that adsorption time did not appear to have any influence on the relationship between interfacial tension and coverage tends to indicate no cross-linking occurs during the ~12 h maximum time frames of these experiments with asphaltene laden interfaces. Furthermore, the fact that the interfacial tension isotherm was not impacted by the presence of asphaltene nanoaggregates in solution suggests that nanoaggregates do not load onto the oil–water interface unless forced to by some experimental means such as evaporation of the asphaltene-carrying phase at the water surface. This interpretation is supported by the quantitative analysis of

the interfacial tension data, which could be fitted using the Langmuir Equation of State (EoS) with a single parameter, i.e., the surface excess coverage, which is the reciprocal of the molecular area. The derived area suggested 6.2 aromatic rings in agreement with the asphaltenes average core size for many asphaltenes according to the Yen–Mullins model.[15−17] The interpretation of this molecular area in terms of core size presumes that the asphaltene core rests in plane with the water surface and the alkyl peripheral substituents are out of plane as previously established using sum frequency generation spectroscopy on Langmuir–Blodgett films.[18]

A confirmation of these results was obtained by dilatational rheology.[11] Provided that oscillations are fast enough to approach the so-called "limiting" elasticity, plotting elastic modulus versus interfacial tension or surface pressure provides another way to determine the EoS of an adsorbate.[19−22] In the case of asphaltenes, the limiting elasticity versus surface pressure relationship proved to be independent of adsorption conditions while being consistent with the asphaltene core size deduced from the Langmuir EoS.

Using the Langmuir EoS, hypotheses regarding cross-linking arising from results such as slow adsorption kinetics,[23−25] rise of shear elasticity,[26−28] and wrinkling upon contraction[29] could be re-evaluated. For example, the slow long-term evolution of interfacial tension could be explained by steric hindrance between surface, disk-like adsorbates when approaching their packing limit.[12] Compressing asphaltenes covered interfaces beyond this packing limit could cause transition to a soft glassy interface with the loss of the Laplacian shape and the appearance of wrinkles.[14] Finally the shear rheology of densely covered asphaltenes interfaces[14] could be described by a soft glass rheology model.[30−33]

Emulsion stabilization by asphaltenes could also be reinterpreted in the light of these findings. Droplet−droplet coalescence appeared to be prevented for the asphaltene studied when surface coverage reached ~3.5 mg/m^2.[34] If a 750 g/mol average molecular weight for these asphaltenes is used, the coverage is ~3 molecules per nm^2, i.e., 80% of surface excess coverage. In other words asphaltenes would block coalescence close to the two-dimensional packing limit for poly-dispersed disks as is also observed for proteins, nanoparticles, and surfactants.[35−38] Altering asphaltenes solubility in the organic phase would of course change their partitioning between bulk and interface: i.e., a higher bulk concentration would be required to reach the packing limit, which however would be expected to remain at ~3.5 mg/m^2. This explains the results published by Yarranton[6] wherein the mass coverage as measured in emulsions after 24 h rest time was always ~3.5 mg/m^2 irrespective of organic phase composition.

This new theory is appealing in that it establishes a quantitative link between the asphaltene molecular structure, interfacial properties, and emulsion stabilization. It, however, relies on the estimate of the polyaromatic core size from tensiometric measurements. The objective of the present article is to evaluate this methodology by characterizing different asphaltenes samples.

The first sample is petroleum asphaltenes of well-known interfacial conformation and core size (Kuwaiti UG8, ones that have an average 6−7 ring core[16] and have been found to lie with their polyaromatic cores in plane (flat) on the water surface[18]). The second sample is coal asphaltenes, known to have a slightly smaller core size (6 rings) and to contain many fewer aliphatic carbons.[16,39] The third is synthetic asphaltenes. It has been chosen as a molecule comprising a polyaromatic core and some alkyl chains. Regarding core size, it would have been possible to match the six to seven-ring core size to observe if interfacial properties of synthetic asphaltenes matched those of petroleum asphaltenes. One could argue however that the correspondence between surface excess coverage and core size is coincidental and arise from a side-on (cores perpendicular to the interface) orientation with a certain distance between parallel polyaromatic cores. With regard to such an argument, the small core size difference between coal and petroleum asphaltenes would not allow evaluation of the possible configurations. Therefore, we chose to synthesize an asphaltene with a polyaromatic core such that the ratio of its core area to the average core area of petroleum asphaltenes is significantly larger than the ratio of its core width to the average core width of petroleum asphaltenes. Then if the analysis of interfacial properties of synthetic asphaltenes led to a contact area corresponding to its actual core area, the side on orientation would be ruled out. On the other hand the synthetic model asphaltenes should not have been unrealistically large compared to petroleum asphaltenes. A balance was found by

choosing a 13-pericondensed ring core (alkylated hexaperibenzocoronene). It corresponds to a double bond equivalent of 35 which is actually the upper limit observed in petroleum asphaltenes by Fourier transform ion cyclotron resonance spectroscopy.[40−43] The ratio of its core area to that of petroleum asphaltenes is 13/7, whereas the ratio of its core width to that of the most pericondensed seven ring structure is 4/3 (and even less for less condensed seven ring structures). Synthesis and characterization details are provided in Supporting Information.
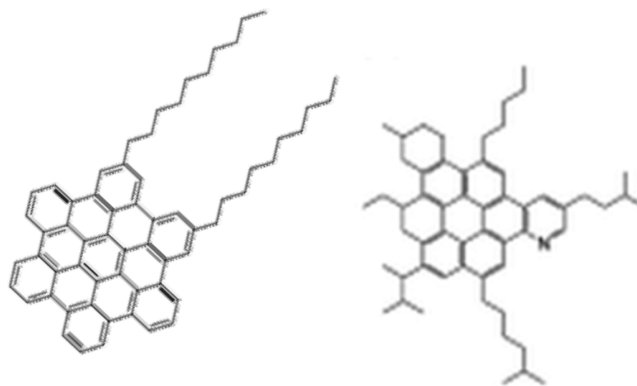

Figure 1. Molecular structure of synthetic asphaltenes alkylated hexaperibenzocoronene (on the left-hand side) versus many petroleum asphaltenes from the Yen−Mullins model (on the right-hand side).

2. MATERIALS AND METHODS

2.1. Chemicals. For the sake of comparison, organic and aqueous phases used in this study are the same as reported in our earlier studies.[10,11] The aqueous phase was deionized Milli-Q grade, with a conductivity of approximately 0.05 μS/cm. It was premixed with 43 g/L of NaCl, and 7 g/L of CaCl$_2$, and the final pH is adjusted to 7 with 0.1 M NaOH to correspond to the water phase used in our previous studies. The organic phase was a 85−15% mixture of an aliphatic oil from the Nexbase oil 2000 series (Neste oil, Finland) and toluene respectively as used in our previous studies.

Petroleum asphaltenes were extracted from Kuwaiti UG8 crude by precipitation with 40 volumes of n-heptane to 1 volume of crude oil, stirring overnight at room temperature, followed by vacuum filtration and rinsing with n-heptane.

Coal-derived asphaltenes were obtained from Indonesia Tanito Harum (TH) coal.[44] The coal was liquefied in a ton/day process-supporting unit (450−465 °C, pressure 16.8 MPa in part from added H$_2$) and distilled. The solid residues from distillation were pulverized to pass through a 60-mesh screen and dried for 2 h under a vacuum at 110 °C. The asphaltene fraction, which is toluene soluble and n-hexane insoluble, was obtained with the Soxhlet extraction technique.

Preparation of synthetic asphaltenes containing a 13-ring core is listed in Supporting Information.

2.2. Interfacial Tension and Pendant Drop As a Langmuir Trough. Interfacial tension of the water−oil interface is investigated using the pendant drop technique (Theta Tensiometer, Biolin Scientific, Finland). Edge detection is used to identify the droplet shape, with the interfacial tension determined using the Young−Laplace equation.[45]

To investigate the relationship between interfacial tension and surface coverage in various adsorption conditions, the pendant droplet apparatus is used to emulate a Langmuir trough following a method developed for surfactants[46,47] and applied to asphaltenes.[10,11] After a certain adsorption time, the droplet is rapidly expanded. Interfacial tension is measured as a function of interfacial area. During rapid area expansion (typically 5 s for a 200% area expansion), it is reasonable to assume that no asphaltenes are exchanged between the bulk and the interface, i.e., $\Gamma(t)\cdot A(t)$ is constant, where $\Gamma(t)$ is the molecular coverage (i.e., the number of molecules per unit area) and $A(t)$ is the surface area

of the droplet at time t. If a reference area is chosen, one can plot interfacial tension vs relative coverage $[\Gamma(t)/\Gamma(A_{ref}) = A_{ref}/A(t)]$ for each test condition. To compare different test conditions (different adsorption times, different asphaltenes mass fraction), a normalization procedure is followed. A common, reference interfacial tension γ_{ref} is chosen that dictates the choice of the reference area, $A_{ref} = A(\gamma_{ref})$ for each test. If adsorbed species undergo relaxation/reorganization over time, or if different species absorb dependent on conditions, then the curves will not overlap but just intersect at $\Gamma(t)/\Gamma(A_{ref}) = 1$. On the contrary if interfacial tension is a unique function of surface coverage, then $\Gamma(A_{ref})$ is constant. In turn, all curves of normalized interfacial tension vs relative coverage $[\Gamma(t)/\Gamma(A_{ref}) = A_{ref}/A(t)]$ will overlap irrespective of the choice of the reference interfacial tension. A "reasonable" reference interfacial tension should be chosen low enough for the uncertainty in the IFT experimental measurements to not generate too high a variability in the reference relative coverage. For example, at low surface pressure (i.e., in the linear regime of the equation of state) an uncertainty of ± 0.2 mN/m for a 2 mN/m reference surface pressure leads to a 10% uncertainty on coverage, which in turn can lead to significant variations of the normalized curves at high surface pressure. Throughout this study a reference surface pressure of 10 mN/m has been chosen.

Further analysis can be performed by comparing the interfacial tension isotherm with various equations of state, and in particular, the Langmuir equation:

$$\gamma(\Gamma) = \gamma_0 + kT\Gamma_\infty \ln(1 - \Gamma/\Gamma_\infty) \qquad (1)$$

where Γ_∞ is surface excess coverage, γ_0 is the clean surface interfacial tension, k is Boltzmann's constant, and T is temperature. $\gamma_0 = 41$ mN/m is known from measurements in the absence of asphaltenes. The remaining unknowns are $\Gamma(A_{ref})$ and Γ_∞ and can be determined by using least squares fitting method.

2.3. Pulsating Drop Experiments. Dilatational rheology experiments were also performed using the pendant droplet technique (PD 200 pulsating drop module in a KSV tensiometer). Area and interfacial tension variations are converted into a complex dilatational modulus defined as

$$E = \frac{d\gamma}{d\ln A} = A\frac{d\gamma}{dA} \qquad (2)$$

From the phase shift between area and interfacial tension oscillations Φ, one can calculate the in-phase, real (elastic), and out-of-phase, imaginary (viscous) moduli:

$$E' = |E|\cos\phi, \quad E'' = |E|\sin\phi \qquad (3)$$

The magnitude of real and imaginary dilatational moduli depends upon the variation of surface coverage during oscillations. If dynamic exchange between bulk solution and interface is slow compared to oscillations, the real modulus will be frequency independent and significantly larger than the imaginary modulus. It then corresponds to the limiting elasticity defined as

$$E_0 = \Gamma\frac{-\partial\gamma}{\partial\Gamma} \qquad (4)$$

For the Langmuir equation of state this yields

$$E_0 = kT\Gamma\left[\frac{\Gamma_\infty}{\Gamma_\infty - \Gamma}\right] \qquad (5)$$

As can be seen, the limiting elasticity is a monotonic function of surface coverage and depends upon the actual value of surface excess coverage. Plotting limiting elasticity versus surface pressure then provides an evaluation of the equation of state.[19−22] Practically, limiting exchanges between bulk and interface can be achieved by using a poor solvent of high viscosity (a 85% of an aliphatic oil with a viscosity greater than 5 cP) and as high an oscillation frequency (∼2 Hz in all cases except in Figure 2) as can be used without leading to hydrodynamic effects. It has been verified throughout our test conditions that the real modulus as measured at 2 Hz is only weakly dependent upon frequency (examples
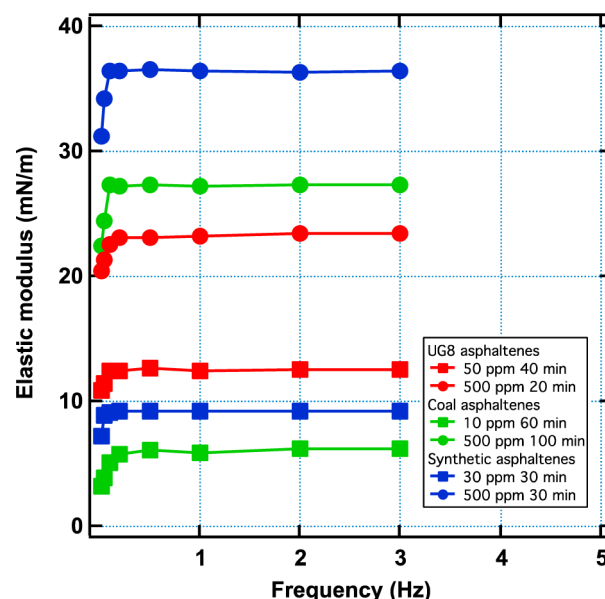

Figure 2. Effect of frequency of oscillation on elastic modulus for different concentrations of all asphaltenes at different aging times.

are given in Figure 2) and is much larger than the imaginary modulus (data not presented here). It has been further verified that hydrodynamic forces due to high viscosity and frequency introduce no bias.[48,49] First, in all test conditions, the profile analysis algorithm is shown fit the droplet shape well. Second, at nearly clean surface conditions (short times, low concentration) the elastic modulus value is always close to the surface pressure value as expected for all equations of state. Third, moduli do not show any amplitude dependence between 2 and 4.5% strain (data not presented here).

3. RESULTS AND DISCUSSION

We will now present and discuss the results obtained for UG8, coal-derived, and synthetic asphaltenes in turn with aging time and bulk concentration being varied widely. As mentioned the data were obtained by the pendant drop method, with the
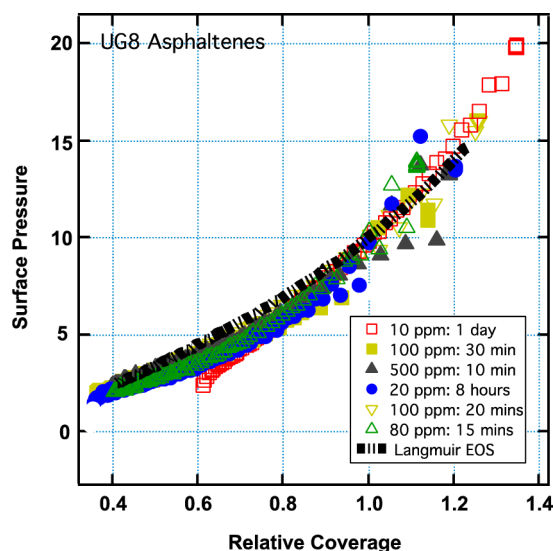

Figure 3. Surface pressure against relative coverage for UG8 asphaltenes for different concentrations and different aging times. A master curve is obtained for all data and is fit by the Langmuir EoS [$\Gamma_\infty = 3.1$ molecules/nm^2].
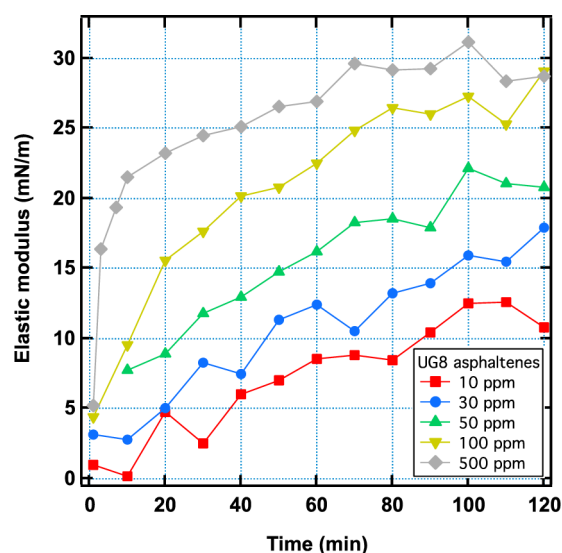
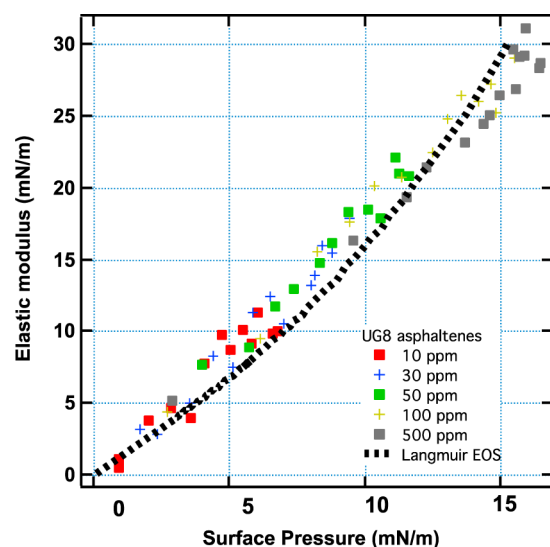**Figure 4.** Time evolution of limiting elasticity for various concentrations of petroleum asphaltenes.

Figure 6. Surface pressure versus relative coverage for coal-derived asphaltenes (different concentrations and different aging times). All data lie on a single master curve fit well by the Langmuir EoS [Γ_∞ = 4.9 molecules/nm^2].

Figure 5. Limiting elasticity versus surface pressure for UG8 asphaltenes and the parametric curve from the Langmuir EoS [Γ_∞ = 3.1 molecules/nm^2].

Figure 7. Time evolution of limiting elasticity for various concentrations of coal-derived asphaltenes.

apparatus being used to emulate a Langmuir trough as well as operated in an oscillation mode to study interfacial rheology.

Figure 3 shows the data of UG8-asphaltene surface pressure against relative coverage $\Gamma(t)/\Gamma(\gamma_{ref}) = A(\gamma_{ref})/A(t)$ obtained during expansion and contraction experiments. Concentrations range from below to above CNAC. Adsorption times prior to area variation range from 15 min to 1 day. As previously observed with petroleum asphaltenes from the Norwegian continental shelf, experimental data largely overlap irrespective of adsorption conditions. As an example contracting a droplet (i.e., increasing coverage) after only 10 min adsorption at 500 ppm yields the same dependency as expanding a droplet (i.e., lowering coverage) after 1 day at 10 ppm. The corresponding master curve can be fairly fitted with the Langmuir EoS, yielding a surface excess coverage of Γ_∞ = 3.1 molecule/nm^2, i.e., a molecular area of 0.32 nm^2 corresponding to the flat on adsorption of a 6.2 ring core. This value is similar to the one previously obtained for asphaltenes from the Norwegian
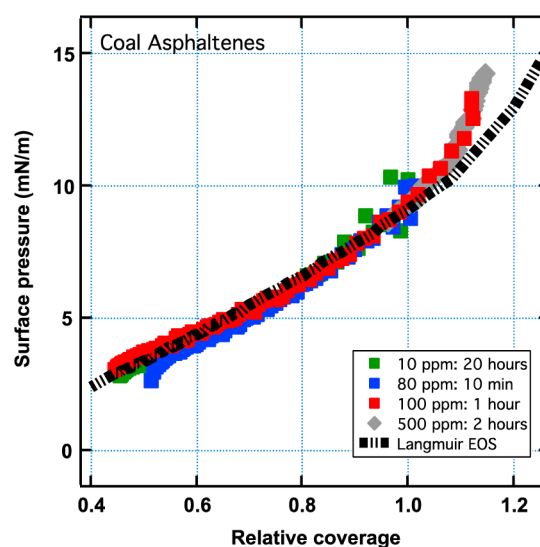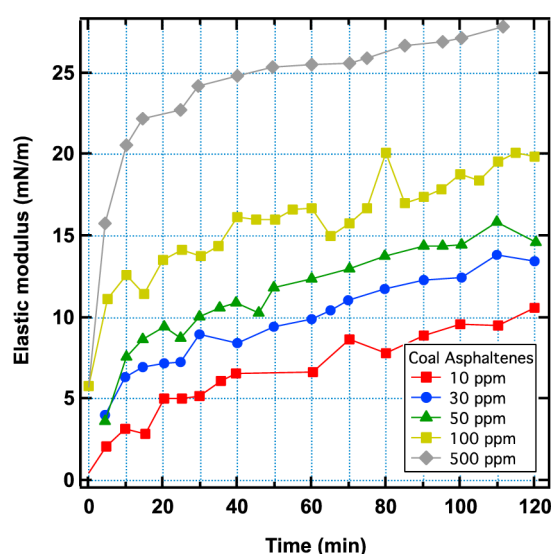
continental shelf[11] and more importantly, very close to the estimate of UG8 aromatic core size (between six and seven rings[16,39]), which are known to rest flat on water.[18]

In addition to contraction/expansion experiments, the evolution of limiting elasticity (as measured at 2 Hz) has been monitored along time with various UG8-asphaltene concentrations as shown in Figure 4. The instantaneous elastic modulus increases with time as asphaltenes accumulate at the interface. The larger the asphaltenes concentration, the faster is the increase of elasticity. Nevertheless when limiting elasticity is plotted versus surface pressure all curves collapse irrespective of adsorption conditions (Figure 5). To be more illustrative let us, for example, observe that 500 ppm after 3 min are equivalent in terms of surface pressure and limiting elasticity to 50 ppm after 2h. Quantitatively the elasticity versus pressure master curve of UG8 asphaltenes superpose to the parametric curve predicted by
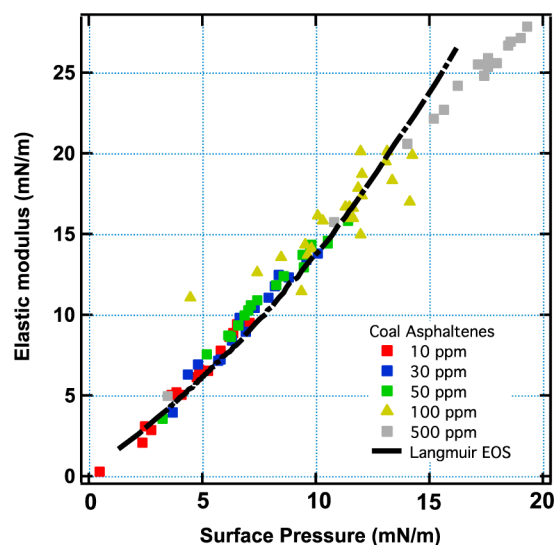
Figure 8. Limiting elasticity versus surface pressure for coal-derived asphaltenes and the parametric curve from the Langmuir EoS [$\Gamma_\infty = 4.9$ molecules/nm^2].

Figure 10. Time evolution of limiting elasticity for various concentrations of coal-synthetic asphaltenes.
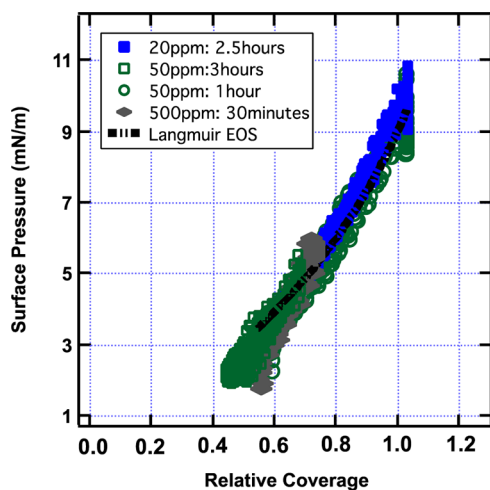

Figure 9. Surface pressure against relative coverage for coal-derived asphaltenes. For different concentrations and different aging times. A single master curve is obtained that is fit well by the Langmuir EoS [$\Gamma_\infty = 1.59$ molecules/nm^2].

Figure 11. Interfacial elastic modulus against surface pressure for synthetic asphaltenes and parametric curve from the Langmuir EoS [$\Gamma_\infty = 1.59$ molecules/nm^2].

Table 1. Comparison of the Mean Number of Rings in Aromatic Cores from Different Measurements

	Mean number of rings in aromatic core from interfacial measurements	Mean number of rings in aromatic core from studies[16,39] or known size
UG8 asphaltenes	6	7
coal-derived asphaltenes	4	5−6
synthetic asphaltenes	12.6	13

the Langmuir EoS [$E_0 = f(\Gamma)$ vs $\gamma = f(\Gamma)$ with $\Gamma_\infty = 3.1$ molecules/nm^2].

Similar results are presented in Figures 6, 7, and 8 for coal-derived asphaltenes (experimental conditions are given in incept). This time the fit by the Langmuir EoS yields a surface excess coverage of 4.9 molecule/nm^2 (0.20 nm^2/molecule), which corresponds to the flat on adsorption of 4 ring core.

Again similar results are presented in Figures 9, 10, and 11 for model asphaltenes (experimental conditions are given in incept). This time the fit by the Langmuir EoS yields a surface excess coverage of 1.59 molecule/nm^2 (0.20 nm^2/molecule), which corresponds to the flat on adsorption of a 12.6 ring core.

Qualitatively the three asphaltenes samples (coal, petroleum, synthetic) behave the same way. Surface pressure and limiting elasticity are functions only of the surface coverage. No effect of aging time can be seen. Quantitatively their behavior can be fairly well represented by the Langmuir EoS with a surface excess coverage corresponding to their actual core size (for synthetic
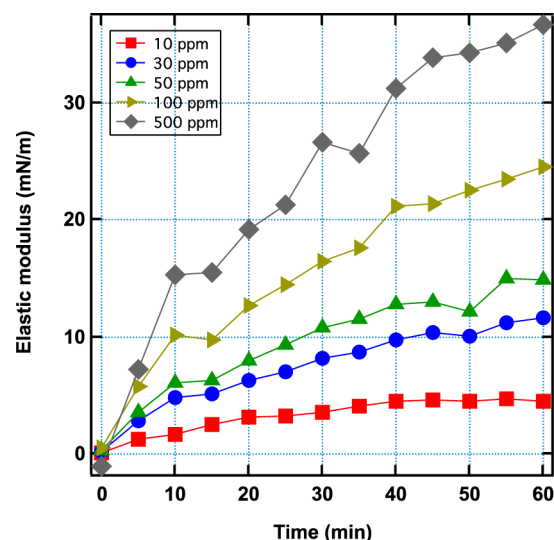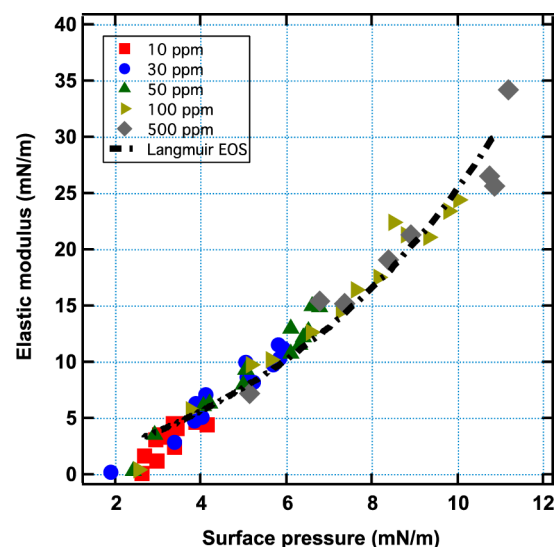
asphaltenes) or estimated average core size (for coal and petroleum). These results confirm the flat on orientation of asphaltenes core at the water surface, similarly to other polyaromatic hydrocarbons at the surface of water and ice.[50−52] This is most probably due to the well documented strong in-plane interactions between polyaromatic hydrocarbons and water molecules or even cations (the so-called lone pair or

cation-π interactions).[53−57] Those interactions exist even for pure hydrocarbons but are enhanced when heteroatoms (such as nitrogen) are substituted into the polyaromatic structure, as in the case in asphaltenes.[58−60]

4. CONCLUSIONS

Previous studies of petroleum asphaltenes from the Norwegian continental shelf at the oil−water interface showed that the surface pressure and the elasticity depend only on the surface coverage and can be well described by the Langmuir EoS with a surface excess coverage corresponding to the flat on adsorption of their aromatic cores. Here, a stringent evaluation of this result was undertaken by comparing coal-derived asphaltenes (∼4 ring core), UG8 petroleum asphaltenes (∼6 ring core) and an alkyl hexabenzocoronene (13-ring core). For all samples, the Langmuir EoS analysis yielded the known core size proving the validity of the finding that the data were captured by this EoS with the surface excess coverage providing a measure of the adsorbed core size. In particular, the well-studied UG8 petroleum asphaltenes exhibit the same molecular area as the Norwegian petroleum asphaltenes and result in sizes that have been independently determined to be very simila.r[16,39]

■ ASSOCIATED CONTENT

ⓈSupporting Information

The Supporting Information is available free of charge on the ACS Publications website at DOI: 10.1021/acs.energy-fuels.5b00179.

■ AUTHOR INFORMATION

Corresponding Author

*E-mail: banerjee@che.ccny.cuny.edu.

Present Address

#Current affiliations for V.P. are Energy Institute, City College of New York and Department of Chemical Engineering, City College of New York.

Notes

The authors declare no competing financial interest.

■ REFERENCES

(1) Sjoblom, J.; Aske, N.; Harald Auflem, I.; Brandal, O.; Erik Havre, T.; Seather, O.; Westvik, A.; Eng Johnsen, E.; Kallevik, H. Our current understanding of water-in-crude oil emulsions.: Recent characterization techniques and high pressure performance. *Adv. Colloid Interface Sci.* **2003**, *100−102* (28), 399−473.

(2) Spiecker, P.; Kilpatrick, P. Interfacial rheology of petroleum asphaltenes at the oil-water interface. *Langmuir* **2004**, *20* (10), 4022−4032.

(3) Bridie, A.; Wanders, T.; Zegveld, W.; Heijde, H. v. d. Formation, prevention and breaking of sea water in crude oil emulsions 'chocolate mousses'. *Mar. Pollut. Bull.* **1980**, *11* (12), 343−348.

(4) Papirer, E.; Bourgeois, C.; Siffert, B.; Balard, H. Chemical nature and water oil emulsifying properties of asphaltenes. *Fuel* **1982**, *61* (8), 732−734.

(5) Rondon, M.; Bouriat, P.; Lachaise, J.; Salager, J. Breaking of water-in-crude oil emulsions. 1. Physicochemical phenomenology of demulsifier action. *Energy Fuels* **2006**, *20* (4), 1600−1604.

(6) Yarranton, H. W.; Hussein, H.; Masliyah, J. H. Water-in-Hydrocarbon Emulsions Stabilized by Asphaltenes at Low Concentrations. *J. Colloid Interface Sci.* **2000**, *228* (1), 52−63.

(7) Siffert, B.; Rageul, P.; Papirer, E. Acid-base characteristics of asphaltenes isolated from mechanical sheared oil distillation residues. *Fuel* **1996**, *75* (14), 1625−1628.

(8) Nordli, K. G.; Sjoblom, J.; Kizling, J.; Stenius, P. Water-in-crude oil emulsions from the Norwegian continental shelf 4. Monolayer properties of the interfacially active crude oil fraction. *Colloids Surf.* **1991**, *57* (1), 83−98.

(9) Sheu, E. Y.; De Tar, M. M.; Storm, D. A.; DeCanio, S. J. Aggregation and kinetics of asphaltenes in organic solvents. *Fuel* **1992**, *71* (3), 299−302.

(10) Rane, J. P.; Harbottle, D.; Pauchard, V.; Couzis, A.; Banerjee, S. Adsorption Kinetics of Asphaltenes at the Oil-Water Interface and Nanoaggregation in the Bulk. *Langmuir* **2012**, *28* (26), 9986−9995.

(11) (a) Rane, J. P.; Pauchard, V.; Couzis, A.; Banerjee, S. Interfacial Rheology of Asphaltenes at Oil-Water Interfaces and Interpretation of the Equation of State. *Langmuir* **2013**, *29* (15), 4750−4759. (b) Rane, Jayant P.; Liang, Xu. Proper Selection of Surfactants for Enhanced Oil Recovery Applications Based on Interfacial Rheology Measurements of Oil-Water Interfaces. *SPE International Symposium on Oilfield Chemistry*; Society of Petroleum Engineers, 2015.

(12) (a) Pauchard, V.; Rane, Jayant P.; Zarkar, S.; Couzis, A.; Banerjee, S. Long term adsorption kinetics of asphaltenes at the oil-water interface: a random sequential adsorption perspective. *Langmuir* **2014**, *30* (28), 8381−8390. (b) Savaji, Kunal; Xue, Li; Couzis, Alexander Understanding the Lateral Movement of Particles Adsorbed At a Solid-Liquid Interface. *J. Colloid Interface Sci.*, 2015. (c) Savaji, Kunal V.; Niitsoo, Olivia; Couzis, Alexander Influence of particle/solid surface zeta potential on particle adsorption kinetics. *J. Colloid Interface Sci.* **2014**, *431*, 165−175.

(13) Rane, J.; Seifert, D.; Andrews, A.; Elshahawi, H.; Dong, C.; Pauchard, V.; Hammond, P.; Zuo, J.; Pomerantz, A.; Banerjee, S.Asphaltene Nanoscience and Reservoir Fluid Gradients, Tar Mat Formation and the Oil-Water Interface. SPE Annual Technical Conference and Exhibition; September 20−October 2, 2013, New Orleans, Louisiana; Society of Petroleum Engineers: Richardson, TX, 2013.

(14) Pauchard, V.; Rane, J. P.; Banerjee, S. Asphaltene-laden interfaces form soft glassy layers in contraction experiments: a mechanism for coalescence blocking. *Langmuir* **2014**, *30*, 12795−12803.

(15) Dutta Majumdar, R.; Gerken, M.; Mikula, R.; Hazendonk, P. Validation of the Yen-Mullins Model of Athabasca Oil-Sands Asphaltenes using Solution-State 1H NMR Relaxation and 2D HSQC Spectroscopy. *Energy Fuels* **2013**, *27* (11), 6528−6537.

(16) Andrews, A. B.; Edwards, J. C.; Pomerantz, A. E.; Mullins, O. C.; Nordlund, D.; Noringa, K. Comparison of Coal-Derived and Petroleum Asphaltenes by 13C Nuclear Magnetic Resonance, DEPT, and XRS. *Energy Fuels* **2011**, *25* (7), 3068−3076.

(17) Zajac, G.; Sethi, N.; Joseph, J. Molecular imaging of petroleum asphaltenes by scanning tunneling microscopy - verification of structure from C-13 and proton nuclear magnetic resonance data. *Scanning Microsc.* **1994**, *8* (3), 463−470.

(18) Andrews, A. B.; McClelland, A.; Korkeila, O.; Demidov, A.; Krummel, A.; Mullins, O. C.; Chen, Z. Molecular Orientation of Asphaltenes and PAH Model Compounds in Langmuir-Blodgett Films Using Sum Frequency Generation Spectroscopy. *Langmuir* **2011**, *27* (10), 6049−6058.

(19) Lucassen, J.; Van Den Tempel, M. Dynamic measurements of dilational properties of a liquid interface. *Chem. Eng. Sci.* **1972**, *27* (6), 1283−1291.

(20) Lucassen-Reynders, E. H.; Cagna, A.; Lucassen, J. Gibbs elasticity, surface dilational modulus and diffusional relaxation in nonionic surfactant monolayers. *Colloids Surf., A* **2001**, *186* (1,Äì2), 63−72.

(21) Lucassen-Reynders, E. H.; Benjamins, J.; Fainerman, V. B. Dilational rheology of protein films adsorbed at fluid interfaces. *Curr. Opin. Colloid Interface Sci.* **2010**, *15* (4), 264−270.

(22) Lucassen-Reynders, E. H.; Fainerman, V. B.; Miller, R. Surface Dilational Modulus or Gibbs' Elasticity of Protein Adsorption Layers. *J. Phys. Chem. B* **2004**, *108* (26), 9173−9176.

(23) Bauget, F.; Langevin, D.; Lenormand, R. Dynamic Surface Properties of Asphaltenes and Resins at the Oil-Air Interface. *J. Colloid Interface Sci.* **2001**, *239* (2), 501−508.

(24) Freer, E. M.; Radke, C. J. Relaxation of asphaltenes at the toluene/water interface: diffusion exchange and surface rearrangement. *J. Adhes.* **2004**, *80* (6), 481−496.

(25) Jeribi, M.; Almir-Assad, B.; Langevin, D.; Henaut, I.; Argillier, J. Adsorption kinetics of asphaltenes at liquid interfaces. *J. Colloid Interface Sci.* **2002**, *256* (2), 268−272.

(26) Fan, Y.; Simon, S.; Sjoblom, J. Interfacial shear rheology of asphaltenes at oil‚Äìwater interface and its relation to emulsion stability: Influence of concentration, solvent aromaticity and nonionic surfactant. *Colloids Surf., A* **2010**, *366* (1−3), 120−128.

(27) Yang, X.; Verruto, V. J.; Kilpatrick, P. K. Dynamic Asphaltene, Resin Exchange at the Oil/Water Interface: Time-Dependent W/O Emulsion Stability for Asphaltene/Resin Model Oils. *Energy Fuels* **2007**, *21* (3), 1343−1349.

(28) Verruto, V. J.; Le, R. K.; Kilpatrick, P. K. Adsorption and Molecular Rearrangement of Amphoteric Species at Oil-Water Interfaces. *J. Phys. Chem. B* **2009**, *113* (42), 13788−13799.

(29) Strassner, J. E. Effect of pH on Interfacial Films and Stability of Crude Oil-Water Emulsions. *J. Pet. Technol.* **1968**, *20*, 303−312.

(30) Fielding, S. M.; Sollich, P.; Cates, M. E. Aging and rheology in soft materials. *J. Rheol.* **2000**, *44* (2), 323−369.

(31) Sollich, P.; Lequeux, F. o.; H√©braud, P.; Cates, M. E. Rheology of Soft Glassy Materials. *Phys. Rev. Lett.* **1997**, *78* (10), 2020−2023.

(32) Sollich, P. Rheological constitutive equation for a model of soft glassy materials. *Phys. Rev. E* **1998**, *58* (1), 738−759.

(33) Bonn, D.; Coussot, P.; Huynh, H.; Bertrand, F.; Debregeas, G. Rheology of soft glassy materials. *EPL* **2002**, *59* (5), 786.

(34) Pauchard, V.; Roy, T. Blockage of coalescence of water droplets in asphaltenes solutions: A jamming perspective. *Colloids Surf., A* **2014**, *443* (0), 410−417.

(35) Pawar, A. B.; Caggioni, M.; Ergun, R.; Hartel, R. W.; Spicer, P. T. Arrested coalescence in Pickering emulsions. *Soft Matter* **2011**, *7* (17), 7710−7716.

(36) Arditty, S.; Whitby, C. P.; Binks, B. P.; Schmitt, V.; Leal-Calderon, F. Some general features of limited coalescence in solid-stabilized emulsions. *Eur. Phys. J. E* **2003**, *11* (3), 273−281.

(37) Tcholakova, S.; Denkov, N. D.; Sidzhakova, D.; Ivanov, I. B.; Campbell, B. Interrelation between Drop Size and Protein Adsorption at Various Emulsification Conditions. *Langmuir* **2003**, *19* (14), 5640−5649.

(38) Fischer, E. K.; Harkins, W. D. Monomolecular Films. The Liquid-Liquid Interface and the Stability of Emulsions. *J. Phys. Chem.* **1931**, *36* (1), 98−110.

(39) Groenzin, H.; Mullins, O. C. Molecular Size and Structure of Asphaltenes from Various Sources. *Energy Fuels* **2000**, *14* (3), 677−684.

(40) Pereira, T. M. C.; Vanini, G.; Oliveira, E. C. S.; Cardoso, F. M. R.; Fleming, F. P.; Neto, A. C.; Lacerda, V., Jr.; Castro, E. q. V. R.; Vaz, B. G.; Romão, W. An evaluation of the aromaticity of asphaltenes using atmospheric pressure photoionization Fourier transform ion cyclotron resonance mass spectrometry, APPI(±)FT-ICR MS. *Fuel* **2014**, *118* (0), 348−357.

(41) Cho, Y.; Kim, Y. H.; Kim, S. Planar Limit-Assisted Structural Interpretation of Saturates/Aromatics/Resins/Asphaltenes Fractionated Crude Oil Compounds Observed by Fourier Transform Ion Cyclotron Resonance Mass Spectrometry. *Anal. Chem.* **2011**, *83* (15), 6068−6073.

(42) Klein, G. C.; Kim, S.; Rodgers, R. P.; Marshall, A. G.; Yen, A. Mass Spectral Analysis of Asphaltenes. II. Detailed Compositional Comparison of Asphaltenes Deposit to Its Crude Oil Counterpart for Two

Geographically Different Crude Oils by ESI FT-ICR MS. *Energy Fuels* **2006**, *20* (5), 1973−1979.

(43) Gaspar, A.; Zellermann, E.; Lababidi, S.; Reece, J.; Schrader, W. Characterization of Saturates, Aromatics, Resins, and Asphaltenes Heavy Crude Oil Fractions by Atmospheric Pressure Laser Ionization Fourier Transform Ion Cyclotron Resonance Mass Spectrometry. *Energy Fuels* **2012**, *26* (6), 3481−3487.

(44) Ikeda, K.; Sakawaki, K.; Nogami, Y.; Inokuchi, K.; Imada, K. Kinetic evaluation of progress in coal liquefaction in the 1t/d PSU for the NEDOL process. *Fuel* **2000**, *79* (3−4), 373−378.

(45) Barnes, G.; Gentle, I. *Interfacial Science: An Introduction*; Oxford University Press: Oxford, U.K., 2005; p 247.

(46) Kumar, N.; Couzis, A.; Maldarelli, C. Measurement of the kinetic rate constants for the adsorption of superspreading trisiloxanes to an air/aqueous interface and the relevance of these measurements to the mechanism of superspreading. *J. Colloid Interface Sci.* **2003**, *267* (2), 272−285.

(47) Pan, R.; Green, J.; Maldarelli, C. Theory and Experiment on the Measurement of Kinetic Rate Constants for Surfactant Exchange at an Air/Water Interface. *J. Colloid Interface Sci.* **1998**, *205* (2), 213−230.

(48) Freer, E. M.; Wong, H.; Radke, C. J. Oscillating drop/bubble tensiometry: effect of viscous forces on the measurement of interfacial tension. *J. Colloid Interface Sci.* **2005**, *282* (1), 128−132.

(49) Alexandrov, N.; Marinova, K. G.; Danov, K. D.; Ivanov, I. B. Surface dilatational rheology measurements for oil/water systems with viscous oils. *J. Colloid Interface Sci.* **2009**, *339* (2), 545−550.

(50) Wick, C. D.; Chen, B.; Valsaraj, K. T. Computational Investigation of the Influence of Surfactants on the Air‚àìWater Interfacial Behavior of Polycylic Aromatic Hydrocarbons. *J. Phys. Chem. C* **2010**, *114* (34), 14520−14527.

(51) Vacha, R.; Cwiklik, L.; Rezac, J.; Hobza, P.; Jungwirth, P.; Valsaraj, K.; Bahr, S.; Kempter, V. Adsorption of Aromatic Hydrocarbons and Ozone at Environmental Aqueous Surfaces. *J. Phys. Chem. A* **2008**, *112* (22), 4942−4950.

(52) Meszar, Z. E.; Hantal, G. r.; Picaud, S.; Jedlovszky, P. l. Adsorption of Aromatic Hydrocarbon Molecules at the Surface of Ice, As Seen by Grand Canonical Monte Carlo Simulation. *J. Phys. Chem. C* **2013**, *117* (13), 6719−6729.

(53) Keiluweit, M.; Kleber, M. Molecular-Level Interactions in Soils and Sediments: The Role of Aromatic Π-Systems. *Environ. Sci. Technol.* **2009**, *43* (10), 3421−3429.

(54) Tarakeshwar, P.; Kim, K. S.; Brutschy, B. Interaction of the water dimer with Π-systems: A theoretical investigation of structures, energies, and vibrational frequencies. *J. Chem. Phys.* **2000**, *112* (4), 1769−1781.

(55) Egli, M.; Sarkhel, S. Lone Pair-Aromatic Interactions: To Stabilize or Not to Stabilize. *Acc. Chem. Res.* **2007**, *40* (3), 197−205.

(56) Reyes, A.; Fomina, L.; Rumsh, L.; Fomine, S. Are water−aromatic complexes always stabilized due to π−H interactions? LMP2 study. *Int. J. Quantum Chem.* **2005**, *104* (3), 335−341.

(57) Hayashi, N.; Higuchi, H.; Ninomiya, K. X/Π Interactions in Aromatic Heterocycles: Basic Principles and Recent Advances. In *Heterocyclic Supramolecules II*; Matsumoto, K.; Hayashi, N., Eds.; Springer: Berlin, 2009; Vol. 18, pp 103−118.

(58) Mitra-Kirtley, S.; Mullins, O. C.; Van Elp, J.; George, S. J.; Chen, J.; Cramer, S. P. Determination of the nitrogen chemical structures in petroleum asphaltenes using XANES spectroscopy. *J. Am. Chem. Soc.* **1993**, *115* (1), 252−258.

(59) McKenna, A. M.; Purcell, J. M.; Rodgers, R. P.; Marshall, A. G. Identification of Vanadyl Porphyrins in a Heavy Crude Oil and Raw Asphaltene by Atmospheric Pressure Photoionization Fourier Transform Ion Cyclotron Resonance (FT-ICR) Mass Spectrometry. *Energy Fuels* **2009**, *23* (4), 2122−2128.

(60) Scotti, R.; Montanari, L. Molecular Structure and Intermolecular Interaction of Asphaltenes by FT-IR, NMR, EPR. In *Structures and Dynamics of Asphaltenes*; Mullins, O.; Sheu, E., Eds.; Springer: Berlin, 1998; pp 79−113.